The Evolution of the Ultraviolet Background

Jennifer E. Scott
(NRC, NASA/GSFC)

Outline

Methods:
*Proximity Effect: QSOs- line of sight, transverse
galaxies
*Lyman alpha forest transmissivity
*Comparison with calculations

Evolution:
*Intensity
*Spectrum (He II, metals)

Sources:
*Quasars, Faint AGN
*Galaxies
*IGM re-emission
*Structure formation (Miniati et al. 2004)

Motivation

Thermal and ionization history of IGM

$$\varepsilon_{HI} = \int_{\nu_0}^{\infty} \frac{4\pi\, J(\nu)\sigma_{HI}(\nu)}{h\nu}(h\nu - h\nu_0)\,d\nu \ \text{ ergs s}^{-1}$$

$$\Gamma_{HI} = \int_{\nu_0}^{\infty} \frac{4\pi J(\nu)\sigma_{HI}(\nu)}{h\nu}\,d\nu \ \text{ s}^{-1}$$

Constrain sources: quasars versus stars

Evolution of sources

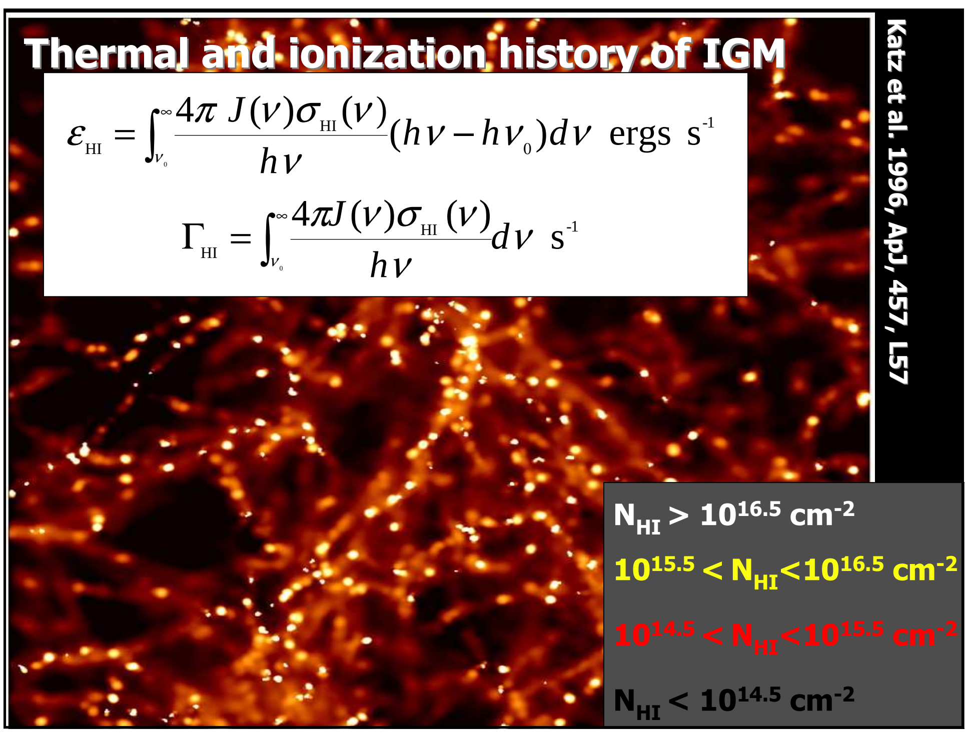

The Proximity Effect

Near a quasar Lyman alpha forest line density modified by quasar's ionizing photons:

$$\frac{dN}{dz} \propto (1+z)^{\gamma} \quad \rightarrow$$

$$\frac{dN}{dz} \propto (1+z)^{\gamma}[1+\omega(z)]^{-(\beta-1)}$$

$z =$ absorber redshift

$$\omega = \frac{F^{Q}(\nu_0)}{4\pi J(\nu_0)} = \frac{\text{quasar flux}}{\text{mean background flux}}$$

Weymann, Carswell, & Smith 1981
Murdoch et al. 1986
Carswell et al. 1987
Bajtlik, Duncan, & Ostriker 1988

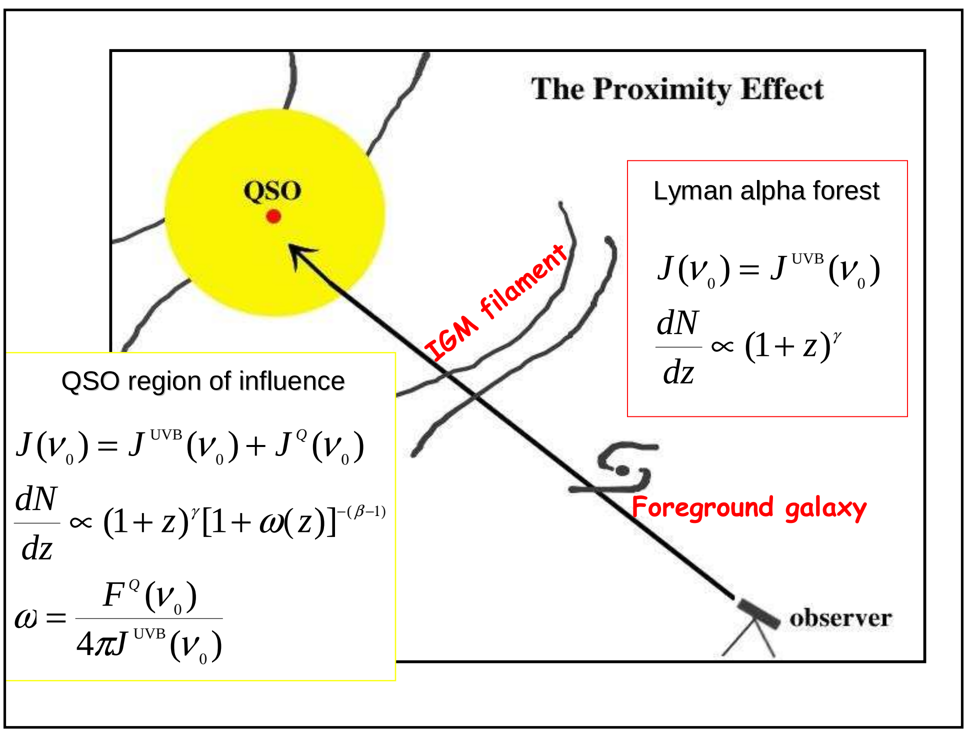

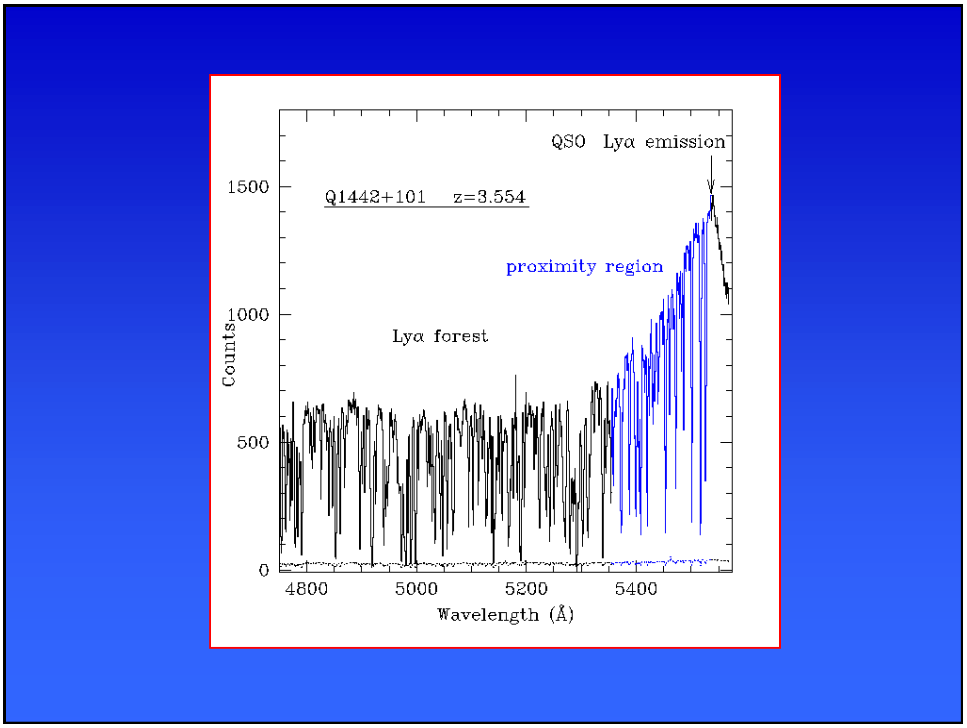
QSO Lyα emission
Q1442+101 z=3.554
proximity region
Lyα forest
Counts
1500
1000
500
0
4800
5000
5200
5400
Wavelength (Å)

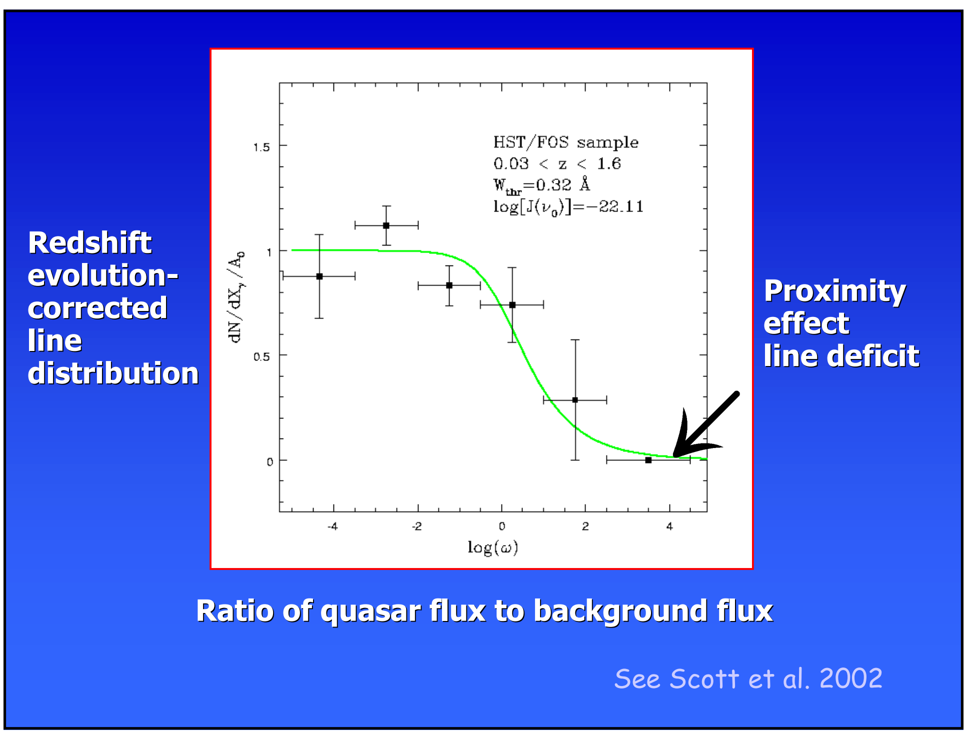
Redshift evolution-corrected line distribution
HST/FOS sample
0.03 < z < 1.6
W_thr=0.32 Å
log[J(ν_0)]=−22.11
dN/dX_γ/A_0
1.5
1
0.5
0
-4
-2
0
2
4
log(ω)
Proximity effect line deficit
Ratio of quasar flux to background flux
See Scott et al. 2002

Systematics

Underestimate
- He, metals
- Dust

Overestimate
- Systemic redshifts
- Curve of growth
- Line Blending
- Lensing
- Clustering/Infall
- Variability

2 < z < 4
mean intensity follows QSO contribution

Z > 4?

Log(mean intensity)

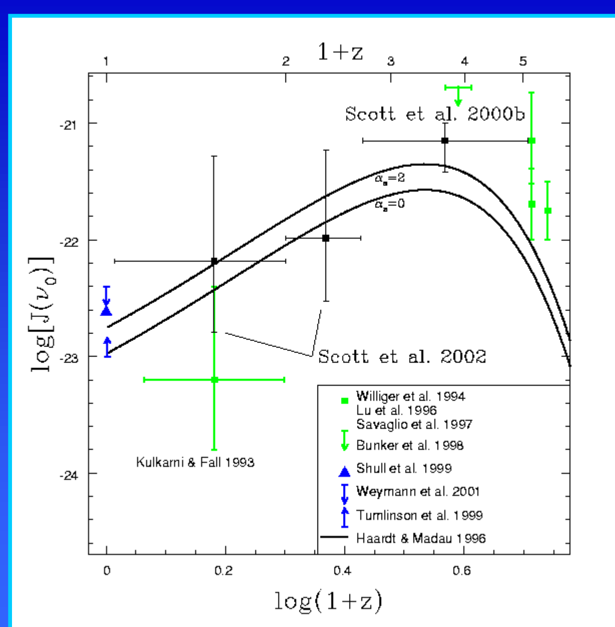

(also Bianchi, Cristiani, & Kim 2001; Sokasian, Abel, & Hernquist 2003)

Transmissivity of Lyman alpha forest

$$\mu \equiv \left(\frac{\Omega_b h^2}{0.0125}\right)\left(\frac{100\ \mathrm{km\,s^{-1}\ Mpc^{-1}}}{H(z)}\right)\Gamma_{-12}^{-1}$$

- Estimate by matching mean flux decrement in hydrodynamical simulations to observations
- Use shape of flux decrement distribution to test cosmological models

Rauch et al. 1997 ApJ, 498, 7

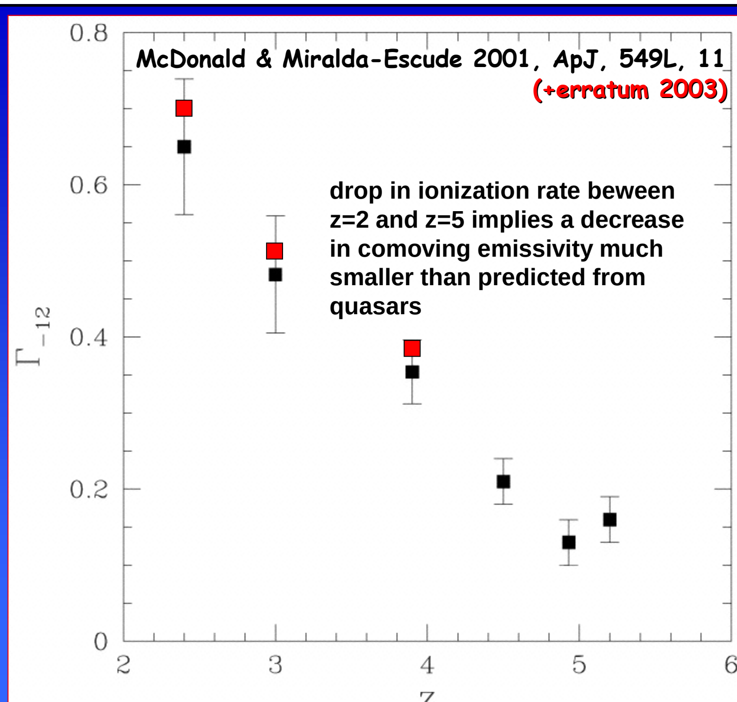

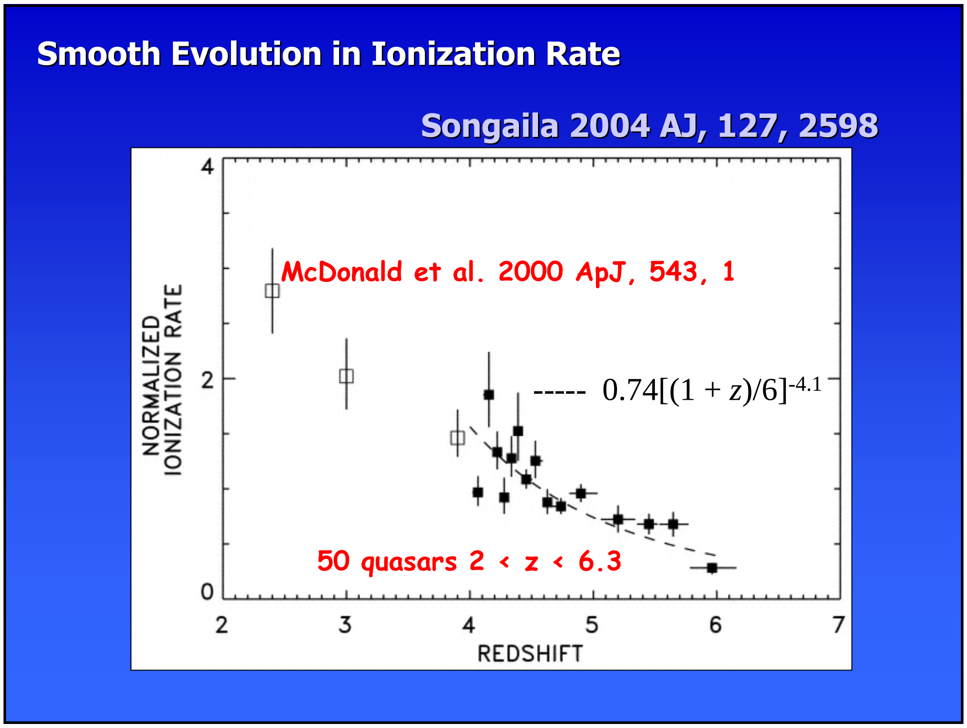
Smooth Evolution in Ionization Rate
Songaila 2004 AJ, 127, 2598
McDonald et al. 2000 ApJ, 543, 1
----- 0.74[(1 + z)/6]^-4.1
50 quasars 2 < z < 6.3
NORMALIZED IONIZATION RATE
REDSHIFT
0
2
4
2
3
4
5
6
7

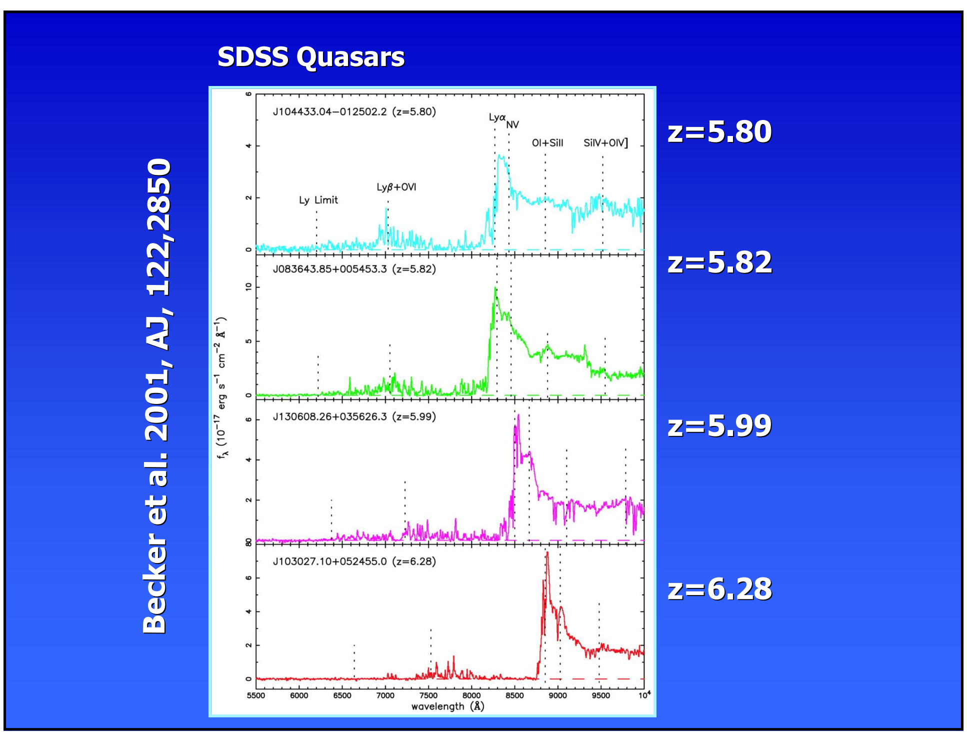
SDSS Quasars
Becker et al. 2001, AJ, 122,2850
J104433.04−012502.2 (z=5.80)
J083643.85+005453.3 (z=5.82)
J130608.26+035626.3 (z=5.99)
J103027.10+052455.0 (z=6.28)
Ly Limit
Lyβ+OVI
Lyα
NV
OI+SiII
SiIV+OIV]
wavelength (Å)
z=5.80
z=5.82
z=5.99
z=6.28

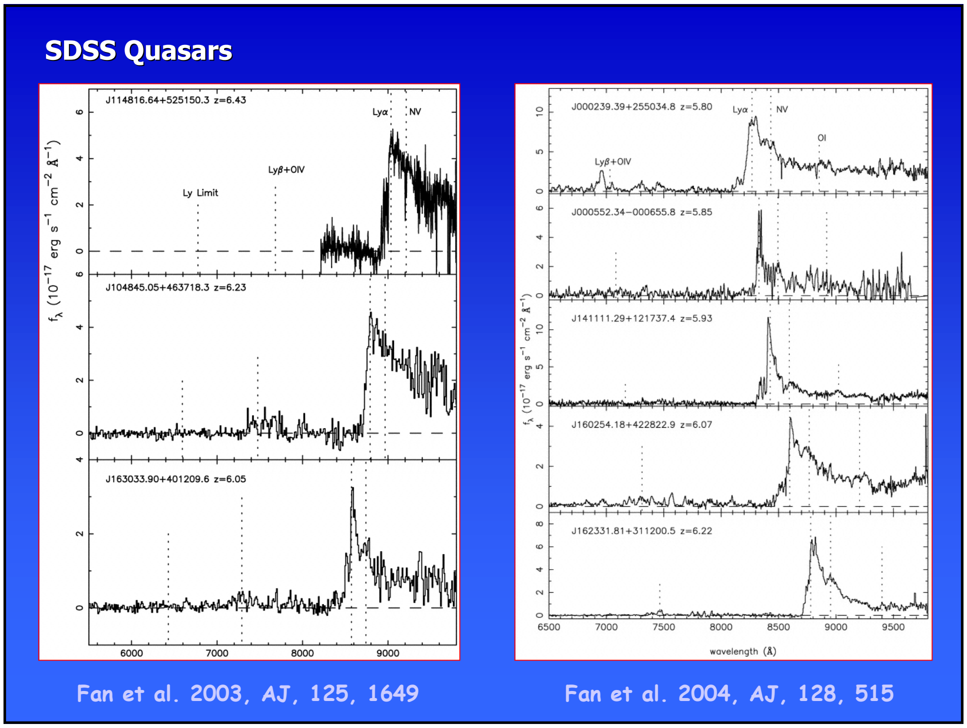
SDSS Quasars
J114816.64+525150.3 z=6.43
J104845.05+463718.3 z=6.23
J163033.90+401209.6 z=6.05
J000239.39+255034.8 z=5.80
J000552.34−000655.8 z=5.85
J141111.29+121737.4 z=5.93
J160254.18+422822.9 z=6.07
J162331.81+311200.5 z=6.22
Ly Limit
Lyβ+OIV
Lyα
NV
OI
wavelength (Å)
Fan et al. 2003, AJ, 125, 1649
Fan et al. 2004, AJ, 128, 515

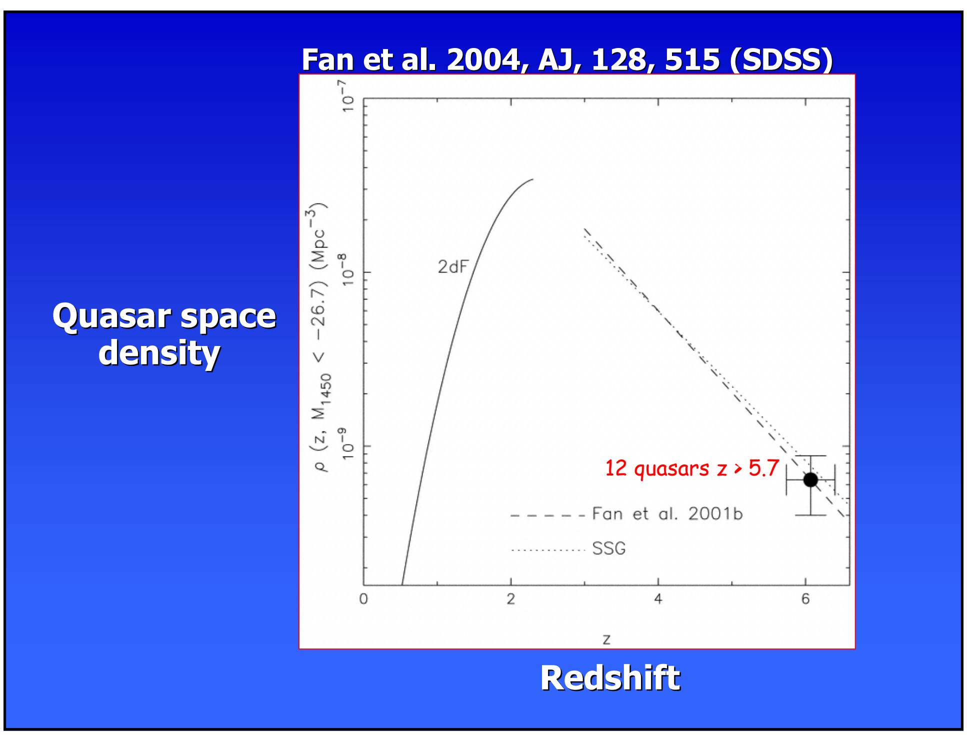
Fan et al. 2004, AJ, 128, 515 (SDSS)
Quasar space density
2dF
12 quasars z > 5.7
Fan et al. 2001b
SSG
z
Redshift

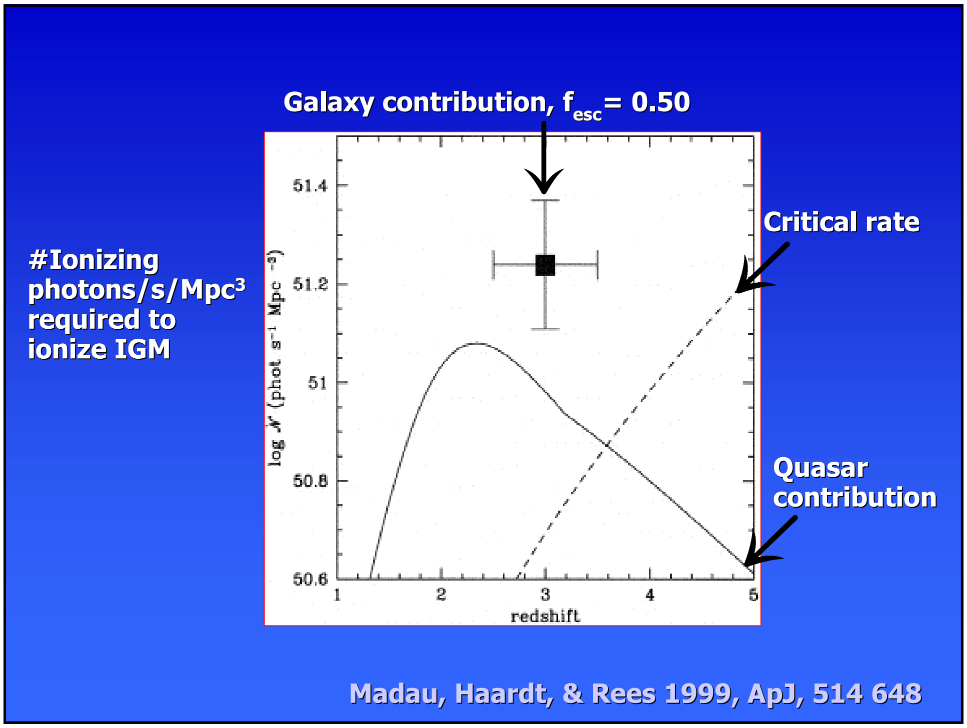
Galaxy contribution, f_esc = 0.50
#Ionizing photons/s/Mpc³ required to ionize IGM
Critical rate
Quasar contribution
log N (phot s⁻¹ Mpc⁻³)
51.4
51.2
51
50.8
50.6
1
2
3
4
5
redshift
Madau, Haardt, & Rees 1999, ApJ, 514 648

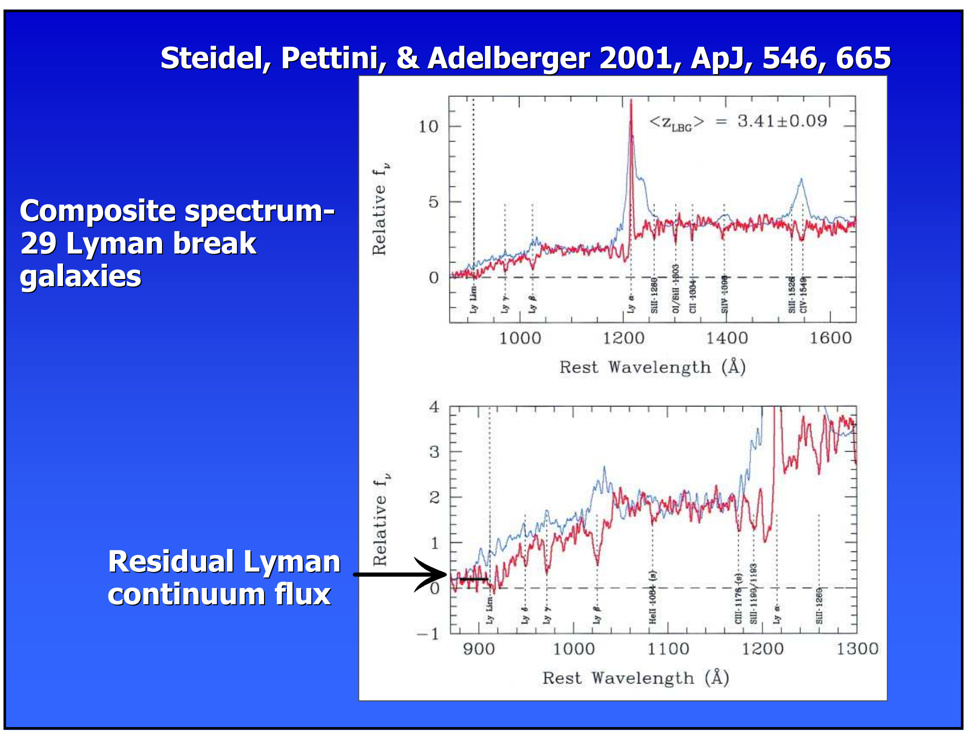
Steidel, Pettini, & Adelberger 2001, ApJ, 546, 665
Composite spectrum-29 Lyman break galaxies
Residual Lyman continuum flux
<z_LBG> = 3.41±0.09
Relative f_ν
Rest Wavelength (Å)
1000
1200
1400
1600
900
1100
1300

However....

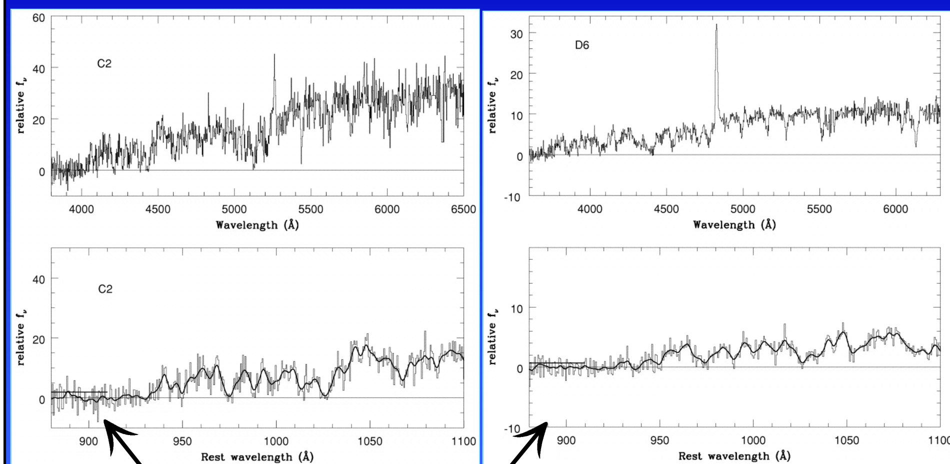

No significant flux

Giallongo et al. 2002, ApJ, 586, L9

Cosmological simulations with radiative transfer - including IGM reemission- require stellar contribution to rise at z > 3 to compensate for drop in quasar space density

Note: Quasar model incorporates increase in L_{min} relative to Seyferts and a soft EUV spectral slope

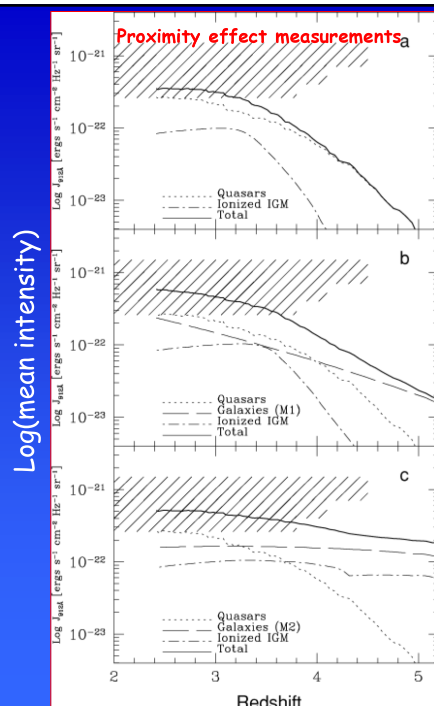

Sokasian, Abel, & Hernquist 2003, MNRAS, 340, 473

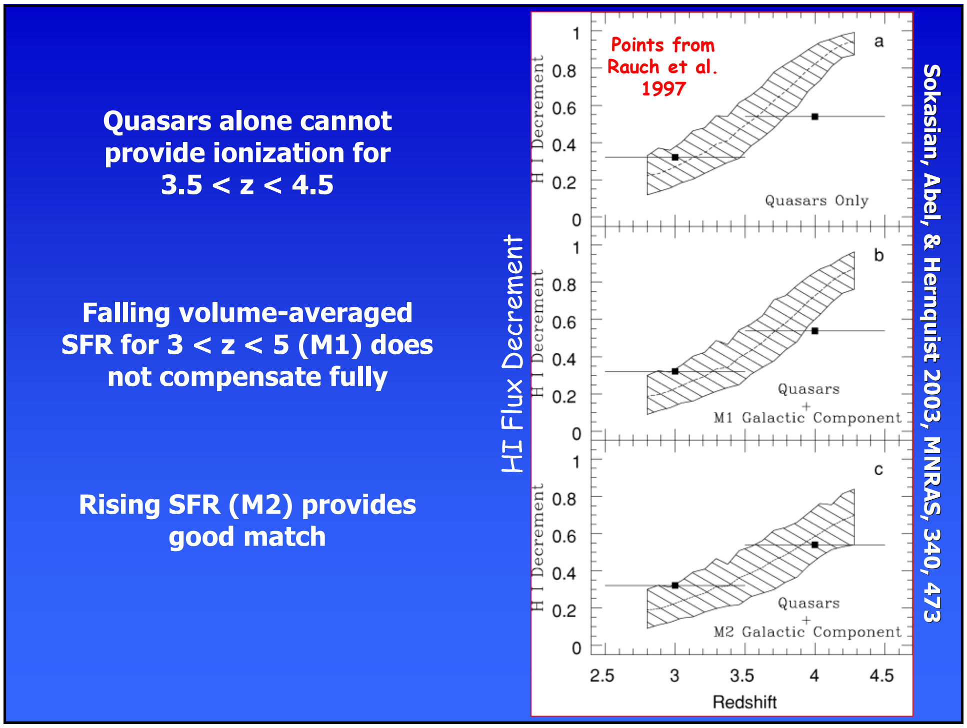
Quasars alone cannot provide ionization for 3.5 < z < 4.5
Falling volume-averaged SFR for 3 < z < 5 (M1) does not compensate fully
Rising SFR (M2) provides good match
HI Flux Decrement
Points from Rauch et al. 1997
Quasars Only
Quasars + M1 Galactic Component
Quasars + M2 Galactic Component
H I Decrement
Redshift
Sokasian, Abel, & Hernquist 2003, MNRAS, 340, 473

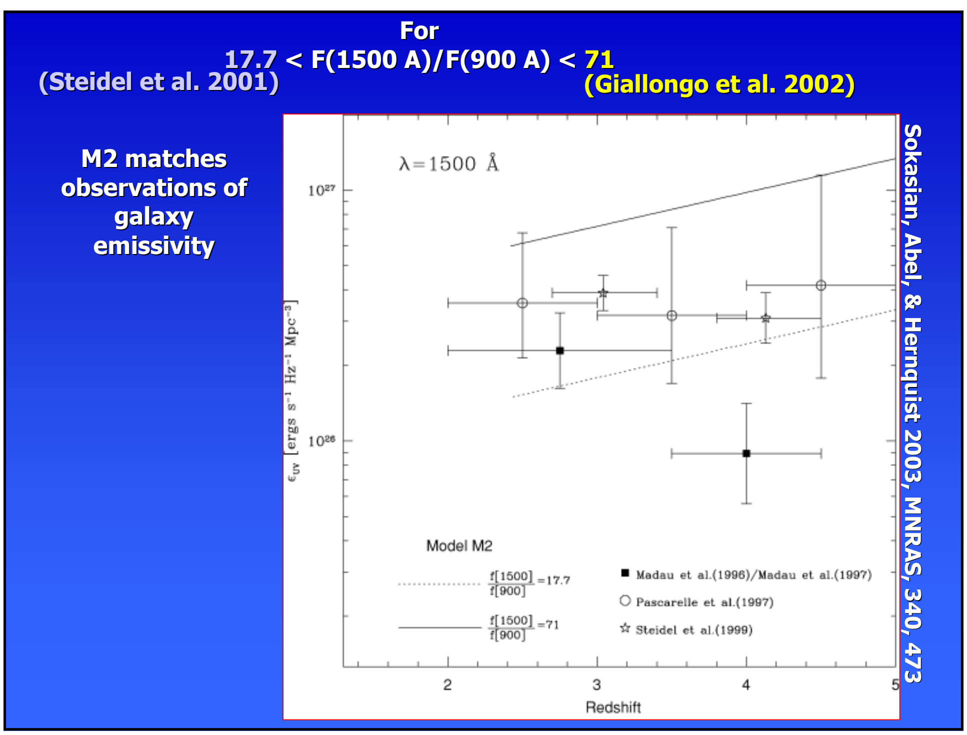
For
17.7 < F(1500 A)/F(900 A) < 71
(Steidel et al. 2001)
(Giallongo et al. 2002)
M2 matches observations of galaxy emissivity
λ=1500 Å
Model M2
Madau et al.(1996)/Madau et al.(1997)
Pascarelle et al.(1997)
Steidel et al.(1999)
Redshift
Sokasian, Abel, & Hernquist 2003, MNRAS, 340, 473

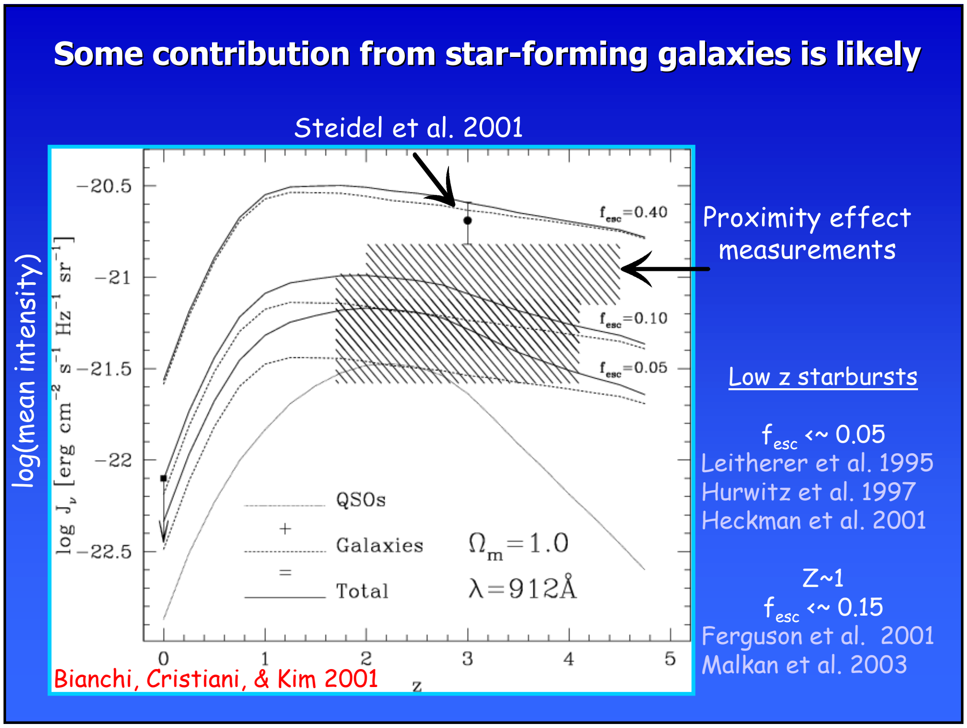
Some contribution from star-forming galaxies is likely
Steidel et al. 2001
Proximity effect measurements
Low z starbursts
f_esc <~ 0.05
Leitherer et al. 1995
Hurwitz et al. 1997
Heckman et al. 2001
Z~1
f_esc <~ 0.15
Ferguson et al. 2001
Malkan et al. 2003
log(mean intensity)
log J_ν [erg cm^-2 s^-1 Hz^-1 sr^-1]
QSOs
Galaxies
Total
Ω_m=1.0
λ=912Å
f_esc=0.40
f_esc=0.10
f_esc=0.05
z
Bianchi, Cristiani, & Kim 2001

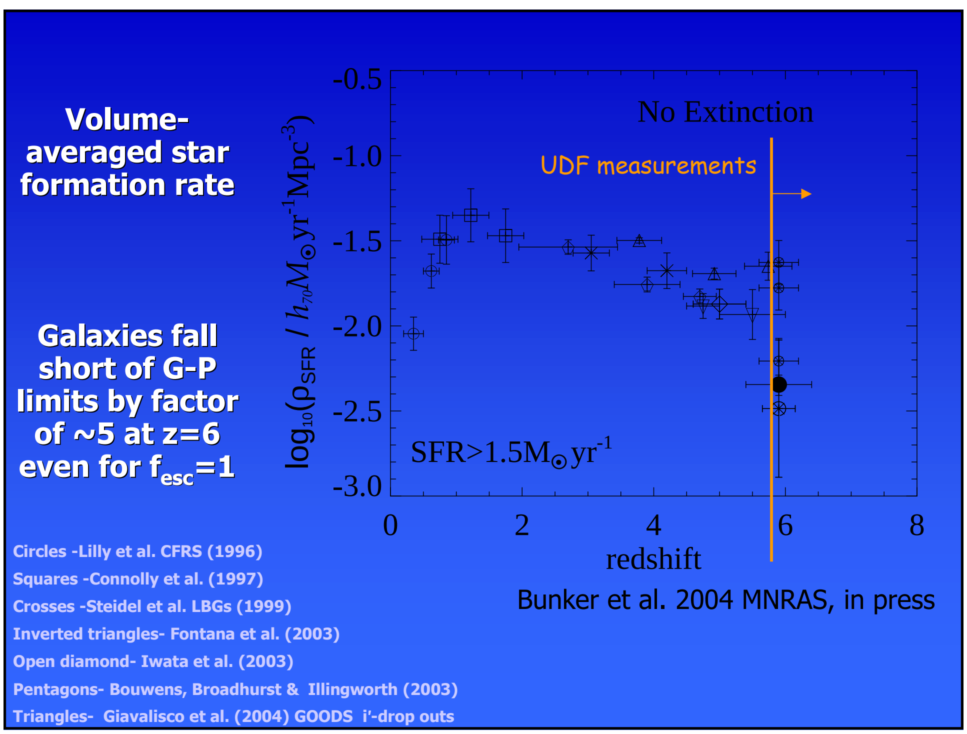
Volume-averaged star formation rate
Galaxies fall short of G-P limits by factor of ~5 at z=6 even for f_esc=1
No Extinction
UDF measurements
SFR>1.5M⊙yr^-1
log10(ρSFR / h70M⊙yr^-1Mpc^-3)
redshift
Bunker et al. 2004 MNRAS, in press
Circles -Lilly et al. CFRS (1996)
Squares -Connolly et al. (1997)
Crosses -Steidel et al. LBGs (1999)
Inverted triangles- Fontana et al. (2003)
Open diamond- Iwata et al. (2003)
Pentagons- Bouwens, Broadhurst & Illingworth (2003)
Triangles- Giavalisco et al. (2004) GOODS i'-drop outs

Contribution of faint AGN

Luminosity function of faint QSOs at z~3

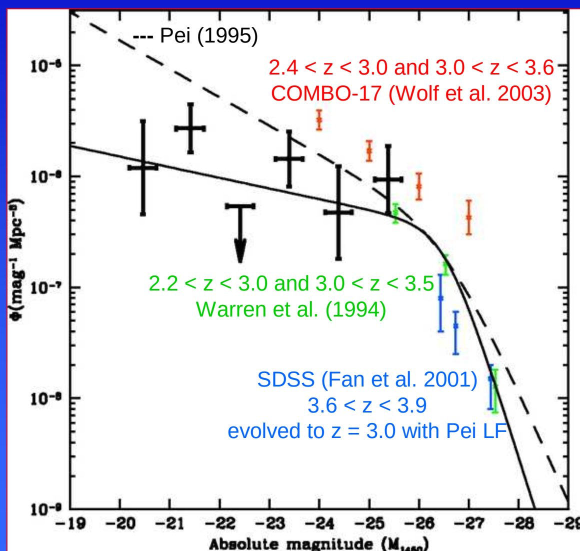

Flatter faint end slope → integrated rest 1450 A luminosity of AGNs is ~1/2 that of previous calculations, and ~8% of LBG contribution at z~3

Upper limit on AGN contribution to UVB

J=2 x 10^{22} egs s^{-1} cm^{-2} Hz^{-1} sr^{-1}

Hunt et al. 2004 ApJ 605, 625

Use observed UVB to constrain faint AGN population

Expected number counts in HDF and Keck AGN surveys

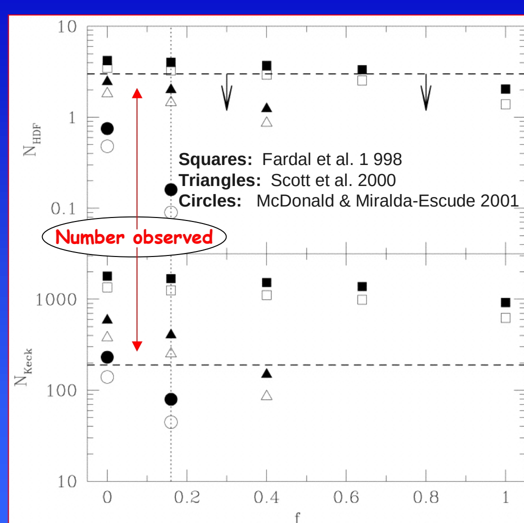

open/filled symbols-with/without contribution from IGM reemission (R = 0.4Q)

- Surveys don't find AGN to supply PE UVB (Squares) even for f_{esc}=1
- Can get agreement w/ lower bound (Triangles) if f_{esc}=0.20
- UVB from <D> (Circles) under-predicts faint AGN counts unless f_{esc} < 0.05

Schirber & Bullock 2003 ApJ 584, 110

Redshift evolution of Lyman-alpha absorbers flattens significantly at low redshift

(Weymann et al. 1998, Kim et al. 2001, Dobrzycki et al. 2002)

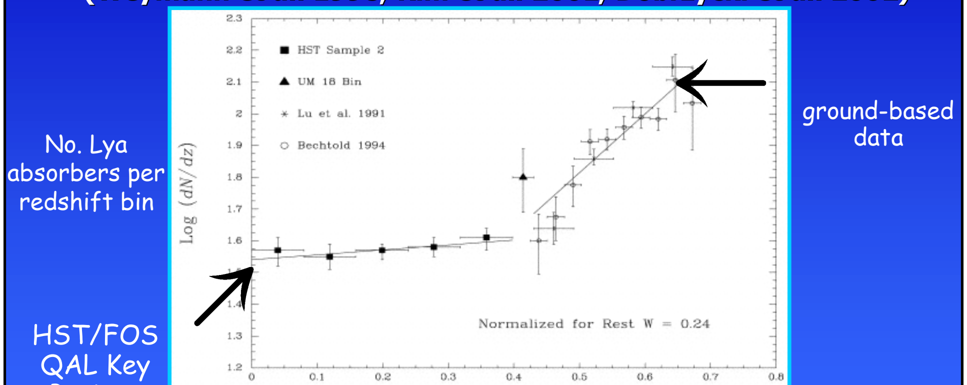

Weymann et al. 1998

$$\frac{\partial n}{\partial z} \propto (1+z)^{\gamma}$$

Evolution driven primarily by evolution in UVB

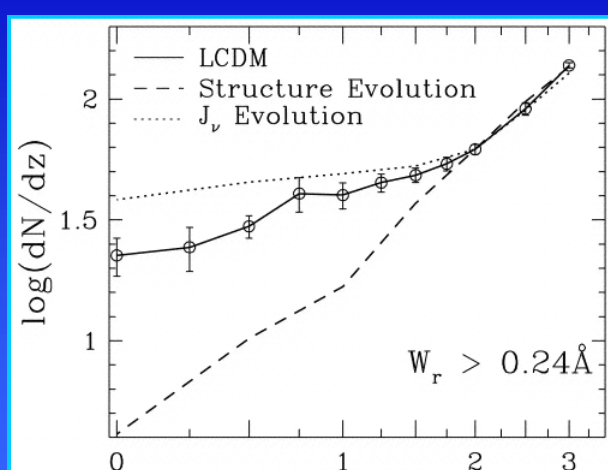

Dave et al. 1999

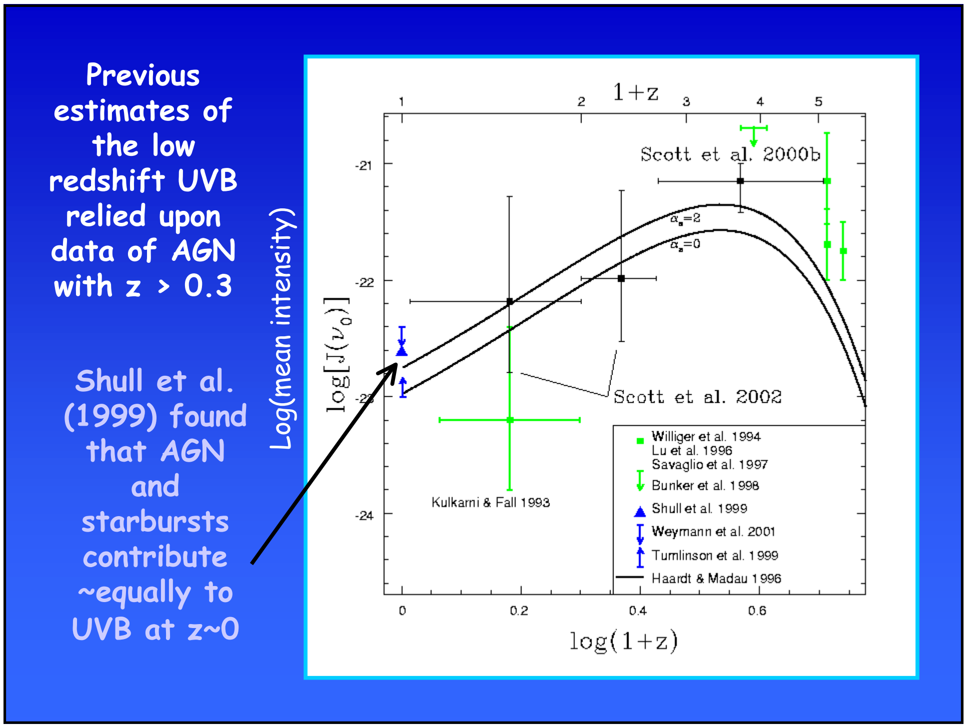
Previous estimates of the low redshift UVB relied upon data of AGN with z > 0.3
Shull et al. (1999) found that AGN and starbursts contribute ~equally to UVB at z~0
Log(mean intensity)
1+z
log[J(ν0)]
log(1+z)
Scott et al. 2000b
Scott et al. 2002
Kulkarni & Fall 1993
Williger et al. 1994
Lu et al. 1996
Savaglio et al. 1997
Bunker et al. 1998
Shull et al. 1999
Weymann et al. 2001
Tumlinson et al. 1999
Haardt & Madau 1996

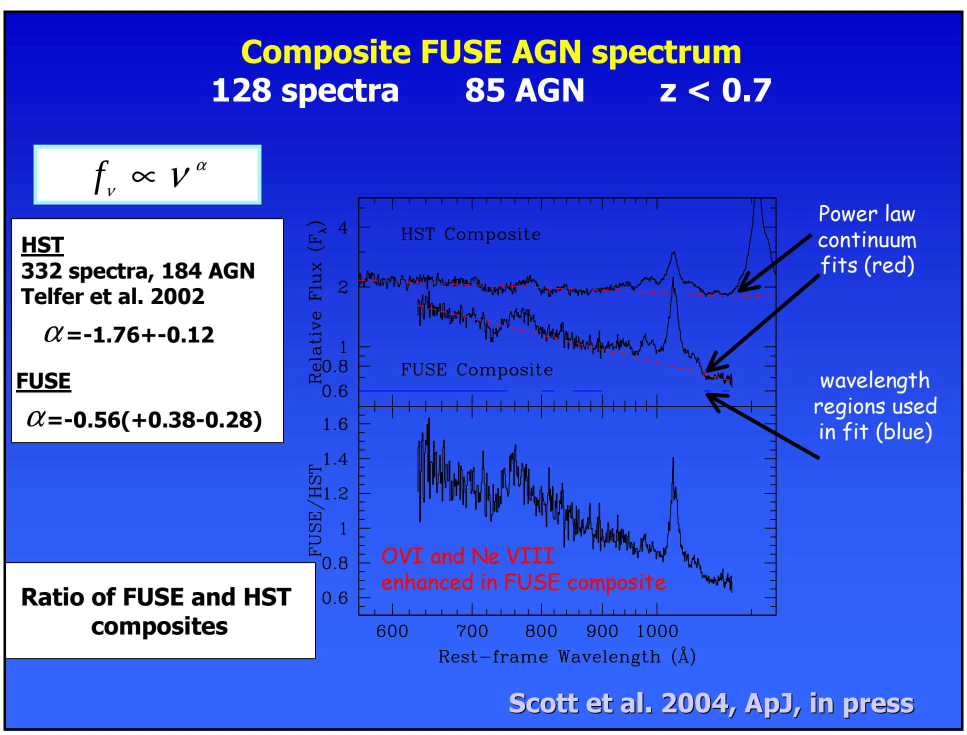
Composite FUSE AGN spectrum
128 spectra 85 AGN z < 0.7
$f_\nu \propto \nu^\alpha$
HST
332 spectra, 184 AGN
Telfer et al. 2002
α=-1.76+-0.12
FUSE
α=-0.56(+0.38-0.28)
Ratio of FUSE and HST composites
HST Composite
FUSE Composite
Relative Flux (Fλ)
FUSE/HST
OVI and Ne VIII enhanced in FUSE composite
Rest-frame Wavelength (Å)
Power law continuum fits (red)
wavelength regions used in fit (blue)
Scott et al. 2004, ApJ, in press

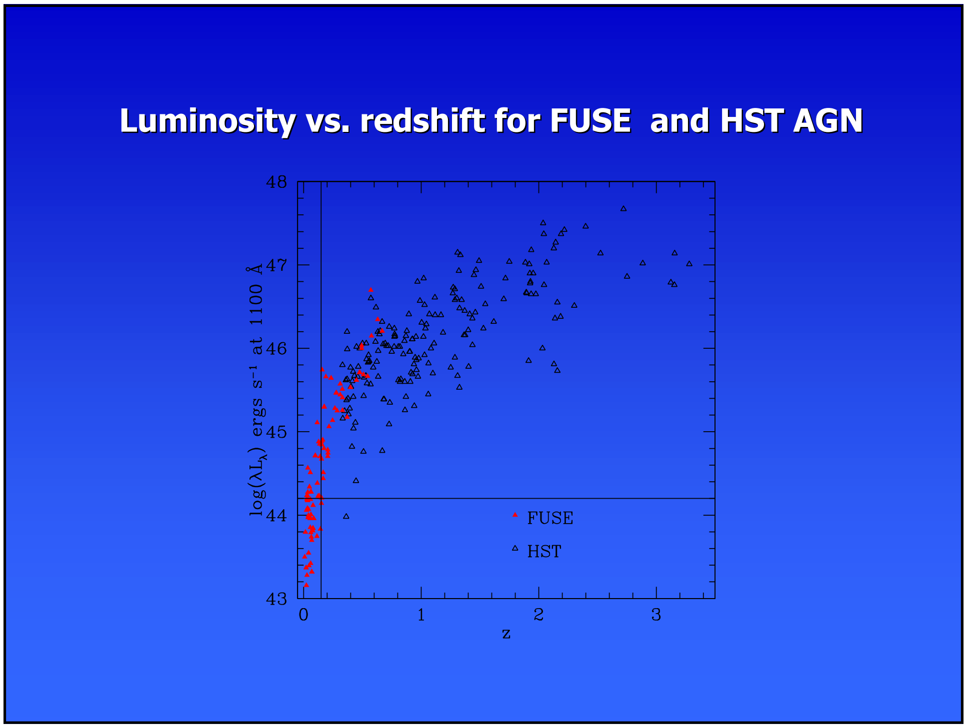
Luminosity vs. redshift for FUSE and HST AGN
log(λL_λ) ergs s⁻¹ at 1100 Å
z
FUSE
HST
43
44
45
46
47
48
0
1
2
3

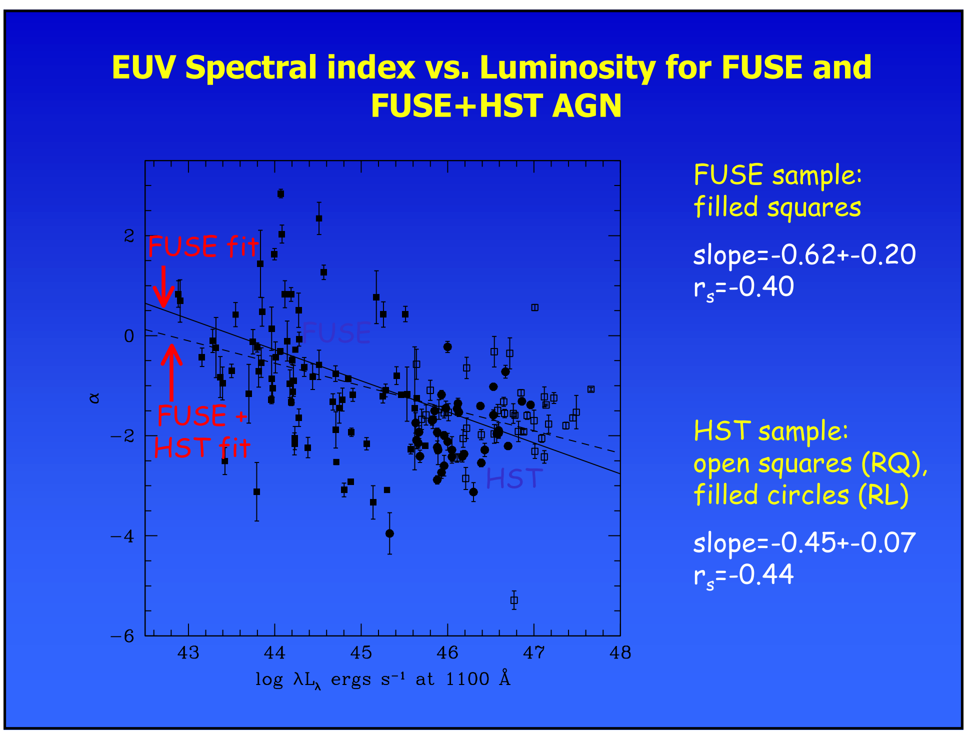
EUV Spectral index vs. Luminosity for FUSE and FUSE+HST AGN
FUSE fit
FUSE + HST fit
FUSE
HST
α
log λL_λ ergs s⁻¹ at 1100 Å
2
0
−2
−4
−6
43
44
45
46
47
48
FUSE sample: filled squares
slope=-0.62+-0.20
r_s=-0.40
HST sample: open squares (RQ), filled circles (RL)
slope=-0.45+-0.07
r_s=-0.44

AGN contribution to UV Background

Observed intensity

Effective opacity of IGM

$$I_\nu \propto \int_{z_{obs}}^{\infty} \frac{dl}{dz} \frac{(1+z_{obs})^3}{(1+z)^3} \varepsilon(\nu,z) \exp(-\tau_{eff}) dz$$

from composite

$$\varepsilon(\nu,z) = \left(\frac{\nu_0}{\nu_B}\right)^{-\alpha_{UV}} \left(\frac{\nu}{\nu_0}\right)^{-\alpha_s} \int \Phi(L,z)$$

Emissivity- depends on EUV spectral index, $alpha_s$ and AGN LF

Shull et al. 1999

Shull et al. 1999

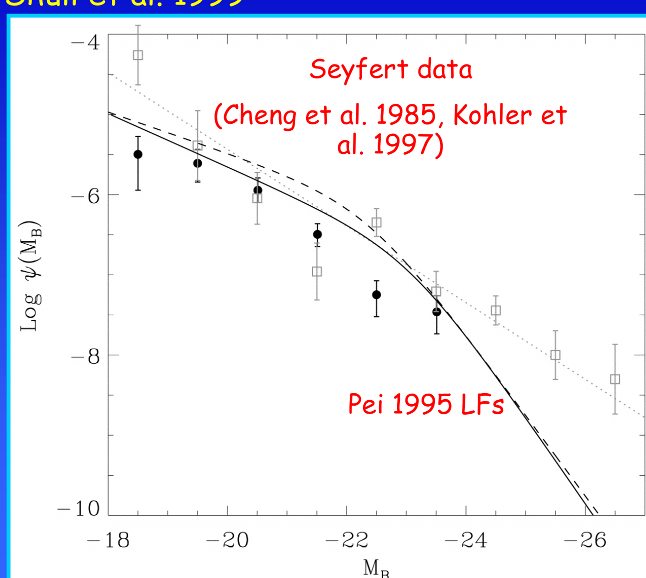

Shull et al. 1999

Differential opacity

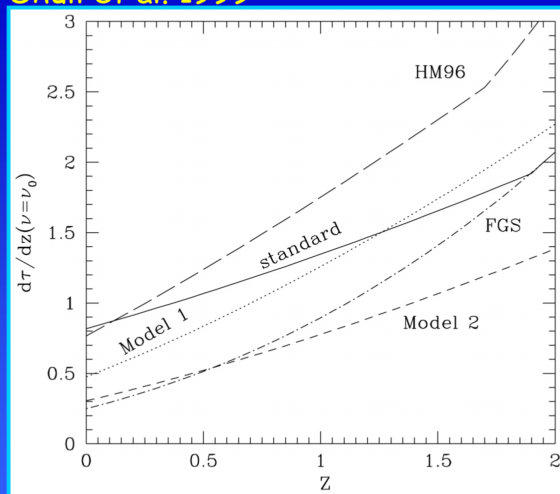

$$\frac{d\tau_{\mathrm{eff}}}{dz} = \int_0^\infty \frac{dn}{dN_{HI}\,dz}[1-\exp(-\tau)]\,dN_{HI}$$

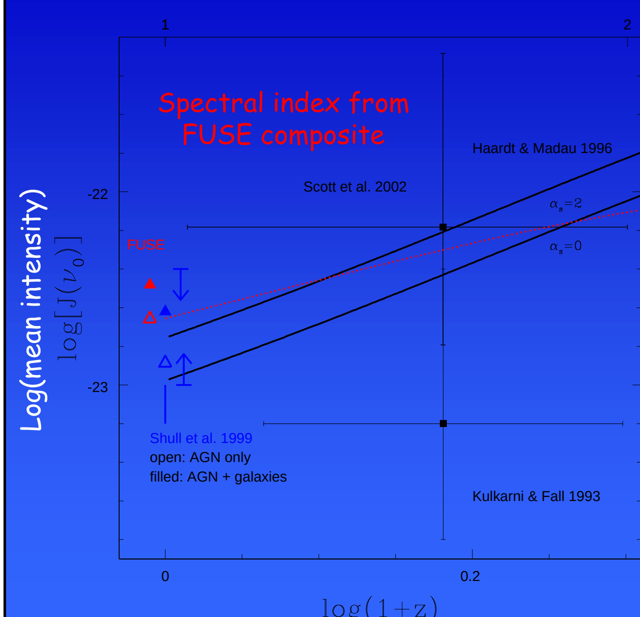

FUSE AGN composite spectrum gives a higher ionizing background at z~0 than the HST QSO composite (alpha~-1.8) by a factor of 1.7

The result is still in good agreement with measurements of the local UV background and with proximity effect estimates of J(912 A)

Spectrum of UVB: He II Absorption 304 A

$$\eta \equiv \frac{\mathrm{N(HeII)}}{\mathrm{N(HI)}}$$ (~20-200 for quasar ionization)

$$= \frac{n(\mathrm{HeII})}{n(\mathrm{HI})} \frac{\alpha_{\mathrm{HeIII}}}{\alpha_{\mathrm{HII}}} \frac{\Gamma_{\mathrm{HI}}}{\Gamma_{\mathrm{HeII}}}$$ For photoionization equilibrium

$$\approx 1.7 \frac{J_{\mathrm{HI}}}{J_{\mathrm{HeII}}} \frac{(3+\alpha_4)}{(3+\alpha_1)} T_{4.3}^{0.055}$$

Measure He II Lya absorption from HST (z > 2.8) or FUSE (z>2) to constrain ratio of UVB intensity or shape at 1 and 4 Ryd

Correlation of N(HeII)/N(HI) with structure in Lya forest

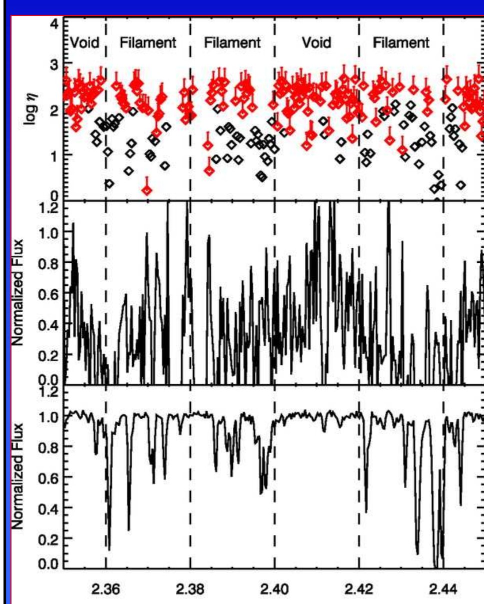

$$f_\nu \propto \nu^{-\alpha_s}$$
$$\langle \alpha_s \rangle = 3.0 \text{ voids}$$
$$\langle \alpha_s \rangle = 1.2 \text{ filaments}$$

Local sources?
IGM filtering?

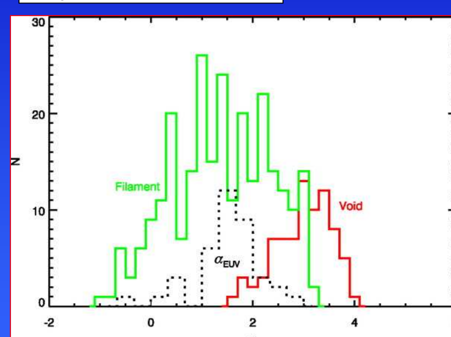

* Radiation at 3-4 Ryd is important for C, Si ionization corrections used to measure IGM metallicty

Shull et al. 2004 ApJ, 600, 570

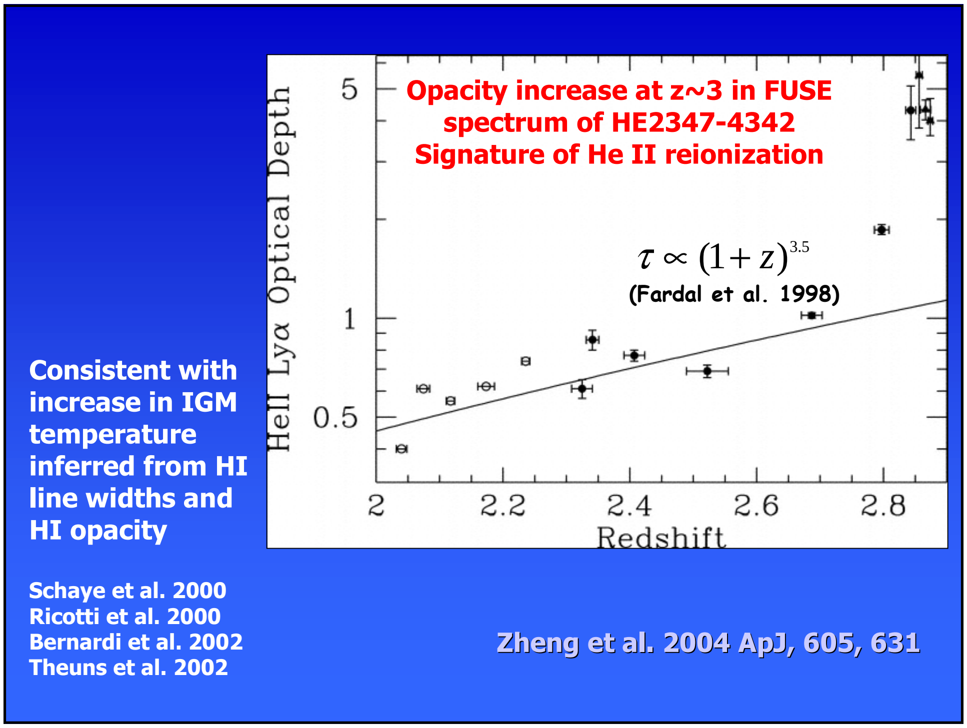
Opacity increase at z~3 in FUSE spectrum of HE2347-4342
Signature of He II reionization
τ ∝ (1+z)^3.5
(Fardal et al. 1998)
HeII Lyα Optical Depth
5
1
0.5
2
2.2
2.4
2.6
2.8
Redshift
Consistent with increase in IGM temperature inferred from HI line widths and HI opacity
Schaye et al. 2000
Ricotti et al. 2000
Bernardi et al. 2002
Theuns et al. 2002
Zheng et al. 2004 ApJ, 605, 631

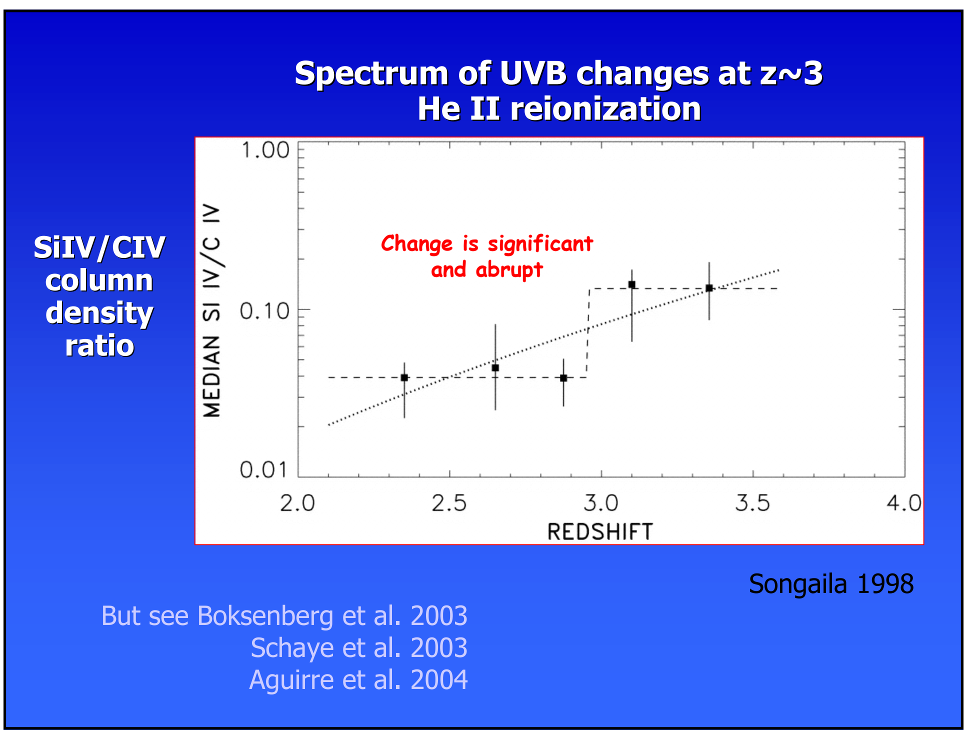
Spectrum of UVB changes at z~3
He II reionization
SiIV/CIV column density ratio
MEDIAN SI IV/C IV
1.00
0.10
0.01
2.0
2.5
3.0
3.5
4.0
REDSHIFT
Change is significant and abrupt
Songaila 1998
But see Boksenberg et al. 2003
Schaye et al. 2003
Aguirre et al. 2004

Transverse Proximity Effect

- Dobrzycki & Bechtold (1991 ApJ 377 L59) found a 10 Mpc void at z=3.17 in HI Lyman alpha forest in Q0302-003 and possible foreground QSO responsible for it
- Heap et al. (2000 ApJ, 534, 69) find high He II opacity at position of D-B void (tau_{HeII}~4.5), indicating local soft source; and report a He II opacity gap at z=3.05-3.07
- Srianand (1997 ApJ, 478, 511) found a 7 Mpc void at z=2.17 in Lya forest of TOL 1038-2712, centered on foreground QSO 4.4 Mpc away; comparison of J with J measured from line of sight PE → foreground QSO was 2-16x brighter ~10^7 yrs ago

Transverse Proximity Effect

- Jakobsen et al. (2003 A&A, 397, 891) find a quasar at z=3.050+-0.003, 3.2 Mpc from line of sight to Q0302-003
- anisotropic emission and t_Q > 10^7 year can account for He II gap

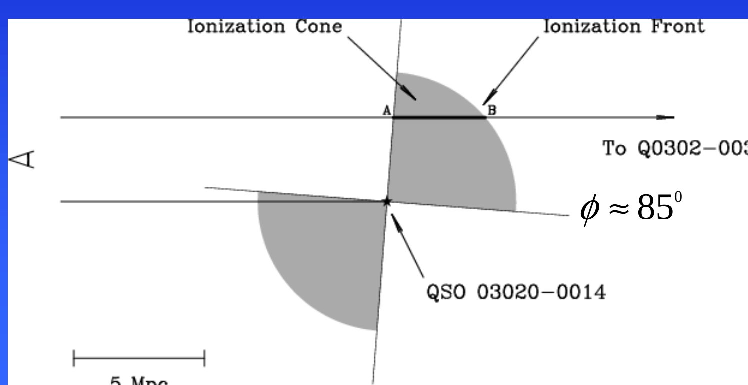

Transverse Proximity Effect

- ESO 2 m, w/WFI + GRISM campaign to search for faint AGN near LOS to bright quasars
- Typically find 3-10 candidates per field (18 fields)

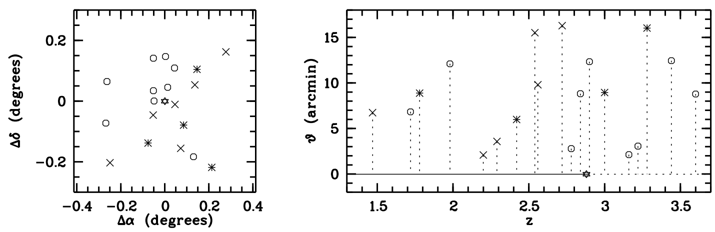

- In Q0302-003 field, find foreground object at redshift of another He II void

L. Wisotzki, G. Worseck, M. Steinmetz, JES, et al.

Transverse Proximity Effect

Croft 2004 ApJ, 610, 642

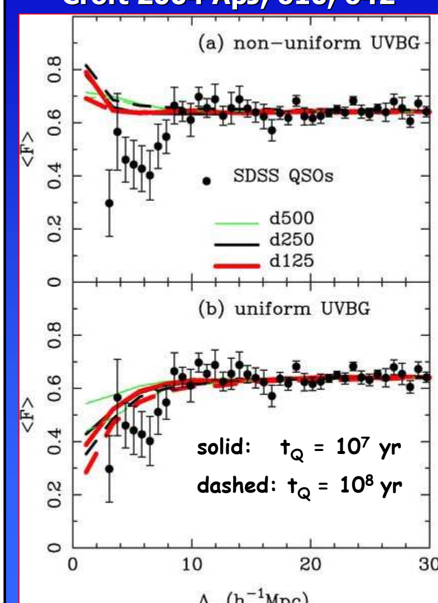

Nbody + hydro + ray tracing to solve radiative transfer

- **Models place quasars in overdense environments and do predict a foreground proximity effect, particularly for a non-uniform UVB**
- **Expect <F> to turn up on scales $r < 2\ h^{-1}$ Mpc (unless UVB is uniform, which is unlikely)**
- **Schirber, Miralda-Escude,& McDonald (2004, ApJ, 610, 105) find no transverse PE in 3 pairs from SDSS EDR**
- **Emission anisotropies require unrealistically small opening angles**
- **Can explain lack of transverse PE by short QSO bursts with 10^4 – 10^6 year timescales**

Adelberger 2004 ApJ 612, 706

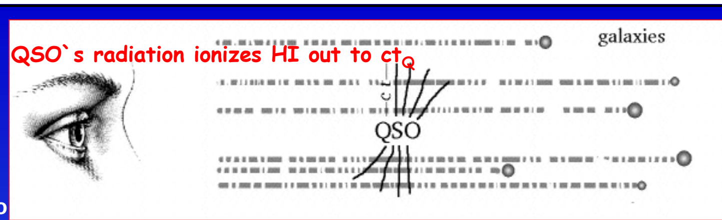

Use galaxy spectra to

(1) map the IGM near the QSO

(2) estimate the geometry of the QSO's region of influence

(3) deduce the QSO's lifetime and emission anisotropy

Galaxies emitting at ∞

Earth at —∞

- At each point, galaxy photons traverse IGM affected by photons emitted by the QSO at different times in the past

- Shaded contours: emission time of the QSO photons that were illuminating a region when the observed photons from a background source passed

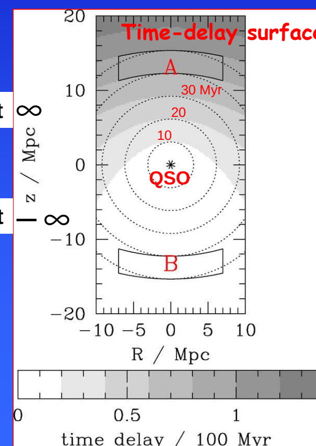

Galaxy Proximity Effect

- Adelberger et al. 2003 (ApJ, 584, 45) found excess HI within 1-5 h^{-1} Mpc of LBGs- large scale structure

- They found an HI deficit within 1 h^{-1} Mpc (especially within 0.5 h^{-1} Mpc)- galaxy proximity effect

- Due to dynamical feedback from SN-driven winds

- Compare to low redshift (Lanzetta et al. 1995, Chen et al. 1998, Pascarelle et al. 2001)

- And to excess absorption near z=2.72 galaxy cB58 (Savagio, Panagia, & Padovani 2002)

Absorption Equiv. Width
-
Impact Parameter
Anti-correlation

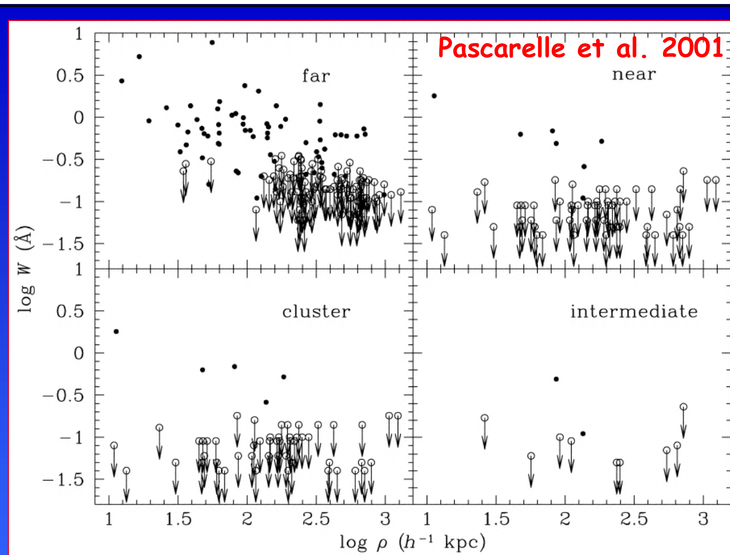

- Galaxies near 24 QSOs (z=0.2-1) show smaller gaseous extent than those far from QSOs
- Galaxies cluster around QSOs causing PE to be underestimated ⟶ J overestimated up to factor of 20

Galaxy Proximity Effect

- **Adelberger et al. 2003 (ApJ, 584, 45) found excess HI within 1-5 h^{-1} Mpc of LBGs- large scale structure**
- **They found an HI deficit within 1 h^{-1} Mpc (especially within 0.5 h^{-1} Mpc)- galaxy proximity effect**
- **Due to dynamical feedback from SN-driven winds**
- **Compare to low redshift (Lanzetta et al. 1995, Chen et al. 1998, Pascarelle et al. 2001)**
- **And to excess absorption near z=2.72 galaxy cB58 (Savaglio, Panagia, & Padovani 2002)**

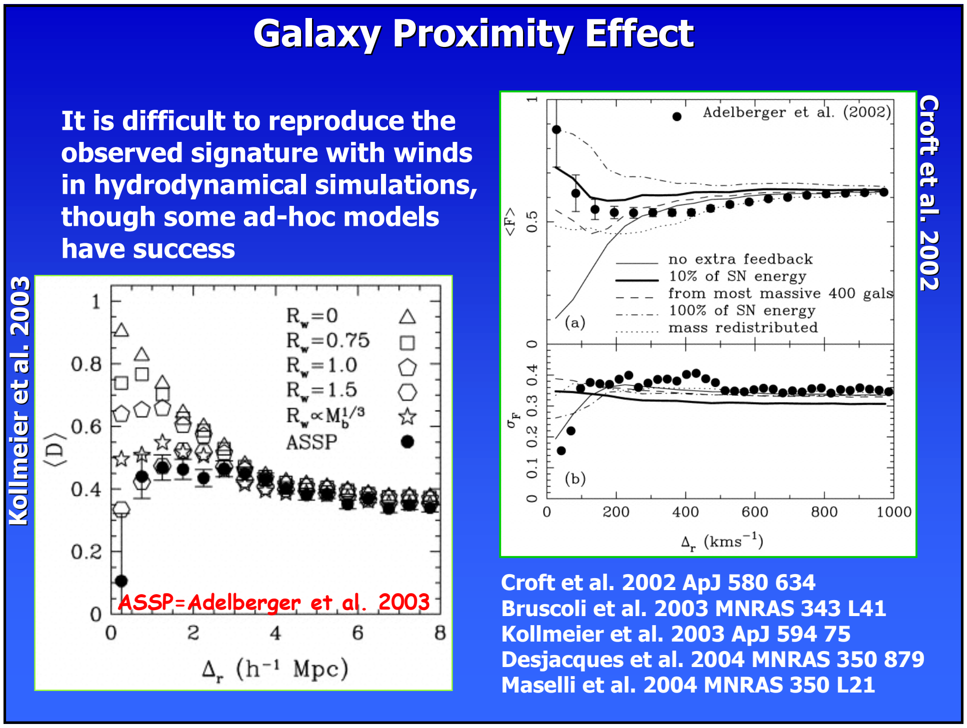
Galaxy Proximity Effect
It is difficult to reproduce the observed signature with winds in hydrodynamical simulations, though some ad-hoc models have success
Kollmeier et al. 2003
R_w=0
R_w=0.75
R_w=1.0
R_w=1.5
ASSP
ASSP=Adelberger et al. 2003
Δr (h⁻¹ Mpc)
Croft et al. 2002
Adelberger et al. (2002)
no extra feedback
10% of SN energy
from most massive 400 gals
100% of SN energy
mass redistributed
Δr (kms⁻¹)
Croft et al. 2002 ApJ 580 634
Bruscoli et al. 2003 MNRAS 343 L41
Kollmeier et al. 2003 ApJ 594 75
Desjacques et al. 2004 MNRAS 350 879
Maselli et al. 2004 MNRAS 350 L21

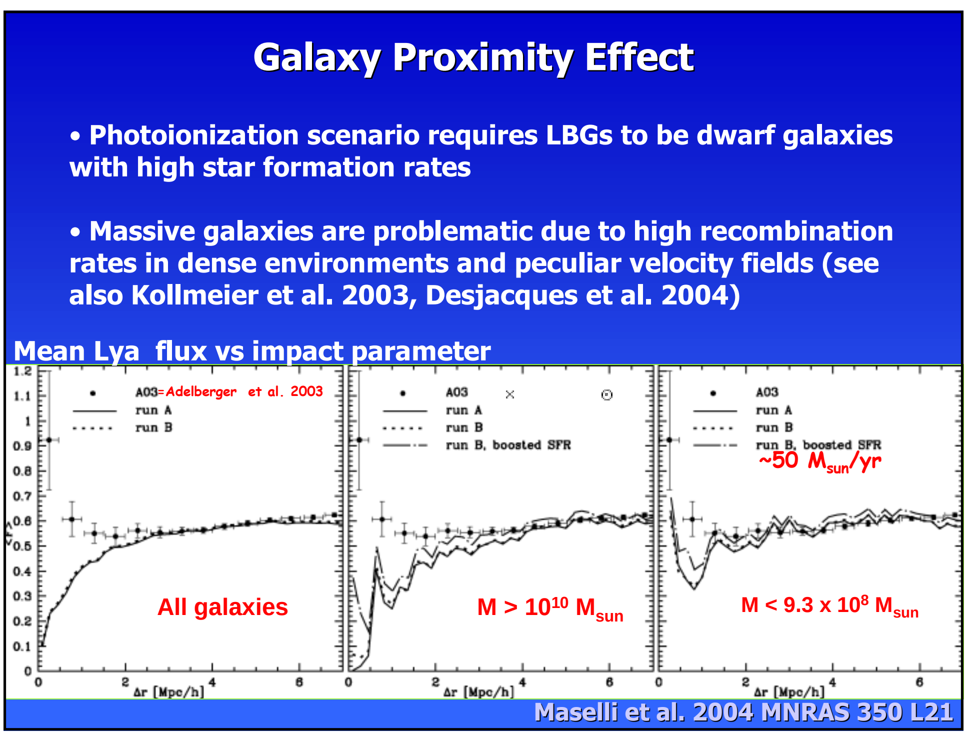
Galaxy Proximity Effect
• Photoionization scenario requires LBGs to be dwarf galaxies with high star formation rates
• Massive galaxies are problematic due to high recombination rates in dense environments and peculiar velocity fields (see also Kollmeier et al. 2003, Desjacques et al. 2004)
Mean Lya flux vs impact parameter
A03=Adelberger et al. 2003
run A
run B
run B, boosted SFR
~50 M_sun/yr
All galaxies
M > 10^10 M_sun
M < 9.3 x 10^8 M_sun
Δr [Mpc/h]
Maselli et al. 2004 MNRAS 350 L21

Summary and Closing Thoughts

- Ionizing Background drops from $z=2$ to $z=0$ driving evolution in Lya forest
- Quasars dominate $z < 3$ (He II reionization) galaxies dominate $z > 3$
- ? Escape fraction from high redshift galaxies
- ? Contribution by faint AGN
- ? Existence of Transverse Proximity effect
- ? Local sources driving variation in N(HeII)/N(HI)
- ? Relative role of photoionization and feedback in Galaxy proximity effect
- Investigate luminosity dependent parameters, eg. AGN spectral slope, galaxy escape fraction (see Ciardi, Bianchi, & Ferrara 2002; Fernandez-Soto, Lanzetta, & Chen 2003)
- Incorporate new QSO luminosity functions for high redshifts (Hunt et al. 2004)